ΤΜΗΜΑ ΙΑΤΡΙΚΗΣ
ΣΧΟΛΗ ΕΠΙΣΤΗΜΩΝ ΥΓΕΙΑΣ
ΠΑΝΕΠΙΣΤΗΜΙΟ ΘΕΣΣΑΛΙΑΣ
ΠΡΟΓΡΑΜΜΑ ΜΕΤΑΠΤΥΧΙΑΚΩΝ ΣΠΟΥΔΩΝ

ΥΠΕΡΗΧΟΓΡΑΦΙΚΗ ΛΕΙΤΟΥΡΓΙΚΗ ΑΠΕΙΚΟΝΙΣΗ ΓΙΑ ΤΗΝ ΠΡΟΛΗΨΗ ΚΑΙ ΔΙΑΓΝΩΣΗ ΤΩΝ ΑΓΓΕΙΑΚΩΝ ΠΑΘΗΣΕΩΝ

Μεταπτυχιακή Διπλωματική Εργασία

"The role of shear wave elastography in the assessment of carotid plaque vulnerability – A Systematic Review and Meta-analysis"

υπό

ΧΡΙΣΤΟΥ Φ. ΠΙΤΡΟΥ

Ειδικευόμενου Αγγειοχειρουργικής

Υπεβλήθη για την εκπλήρωση μέρους των
απαιτήσεων για την απόκτηση του
Διπλώματος Μεταπτυχιακών Σπουδών
«Υπερηχογραφική Λειτουργική Απεικόνιση για την πρόληψη & διάγνωση των αγγειακών παθήσεων»

Λάρισα, 2025

Επιβλέπων:

Σταύρος Κ. Κάκκος, Καθηγητής Αγγειοχειρουργικής, Τμήμα Ιατρικής, Πανεπιστήμιο Πατρών

Τριμελής Εξεταστική Επιτροπή:

1. *Σταύρος Κ. Κάκκος, Καθηγητής Αγγειοχειρουργικής, Τμήμα Ιατρικής, Πανεπιστήμιο Πατρών*
2. *Ιωάννης Κακίσης, Καθηγητής Αγγειοχειρουργικής, Ιατρική Σχολή, Εθνικό και Καποδιστριακό Πανεπιστήμιο Αθηνών*
3. Αθανάσιος Γιαννούκας, Καθηγητής Αγγειοχειρουργικής, Τμήμα Ιατρικής, Πανεπιστήμιο Θεσσαλίας

ΠΕΡΙΕΧΟΜΕΝΑ

Πρόλογος – Ευχαριστίες

Ευχαριστώ θερμά τον καθηγητή κ. Κάκκο Σταύρο, που ως επιβλέποντας της μεταπτυχιακής μου εργασίας με βοήθησε μέσω των πολύτιμων υποδείξεων, συμβουλών και συστάσεων προς την περάτωση αυτής.

Εκφράζω τις ευχαριστίες μου στον Καθηγητή κ. Γιαννούκα Αθανάσιο για την επιλογή μου ως φοιτητή στο ΜΠΣ, δίνοντάς μου έτσι την ευκαιρία να ενισχύσω τις γνώσεις μου στην εφαρμογή του υπερήχου για την πρόληψη και τη διάγνωση των αγγειακών παθήσεων.

Επίσης, θα ήθελα να ευχαριστήσω αλλά και να συγχαρώ τους διδάσκοντες του ΜΠΣ για υψηλό επίπεδο των διαλέξεων.

Τέλος, ευχαριστώ τη γραμματεία του ΜΠΣ για την εύστοχη βοήθεια και άμεση ανταπόκριση καθ' όλη τη διάρκεια του προγράμματος.

Περίληψη

Στόχος: Η εξέταση του ρόλου της ποσοτικοποίησης της σύνθεσης της καρωτιδικής πλάκας με τη χρήση ελαστογραφίας διατμητικών κυμάτων (shear wave elastography, SWE) και της επακόλουθης ταξινόμησης της πλάκας ως ασταθούς, αίτιο αγγειακού εγκεφαλικού επεισοδίου ή ευάλωτης, δηλαδή επιρρεπής για την εμφάνιση αγγειακού εγκεφαλικού επεισοδίου.

Μέθοδοι: Πραγματοποιήθηκε συστηματική ανασκόπηση και μετα-ανάλυση με βάση τη μεθοδολογία «προτιμώμενων στοιχείων αναφοράς για συστηματικές ανασκοπήσεις και μετα-αναλύσεις» (PRISMA). Ο πρωταρχικός στόχος ήταν να αξιολογηθεί το SWE ως διαγνωστικό εργαλείο για τις ασταθείς και ευάλωτες καρωτιδικές πλάκες.

Αποτελέσματα: Η αναζήτηση κατέληξε στον εντοπισμό 606 μελετών, εκ των οποίων οι 24 εξέτασαν συγκεκριμένα τον πρωταρχικό μας στόχο. Πέντε συγκριτικές μελέτες συμπεριλήφθηκαν στην ομάδα συμπτωματικών (ασταθών) έναντι ασυμπτωματικών της μετα-ανάλυσης, ενώ τρείς συμπεριλήφθηκαν στην ομάδα ευάλωτων έναντι σταθερών. Οι ευάλωτες και ασταθείς/συμπτωματικές καρωτιδικές πλάκες εμφάνισαν σημαντικά χαμηλότερες τιμές του συντελεστή του Young (kPa) (και οι δύο, $p <,001$).

Συμπέρασμα: Το SWE έχει δείξει πολλά υποσχόμενα αποτελέσματα για την αξιολόγηση της καρωτιδικής πλάκας και τη διαστρωμάτωση του κινδύνου αγγειακού εγκεφαλικού επεισοδίου. Απαιτούνται περαιτέρω προοπτικές πολυκεντρικές κλινικές μελέτες για τον προσδιορισμό των βέλτιστων τεχνικών και παραμέτρων για τον συντελεστή του Young και της ταχύτητας διατμητικού κύματος, ως δείκτες της SWE, ενισχύοντας την πρωτογενή και δευτερογενή πρόληψη και τη θεραπεία του αγγειακού εγκεφαλικού επεισοδίου.

Λέξεις – κλειδιά: ελαστογραφία, υπέρηχος, καρωτιδική αθηροσκλήρυνση, αγγειακό εγκεφαλικό επεισόδιο

Abstract

Objective: To examine the role of quantification of the carotid plaque's composition using shear wave elastography (SWE) and the subsequent classification of the plaque as unstable, causing a stroke or vulnerable, prior to the occurrence of a stroke.

Methods: A systematic review and meta-analysis were conducted based on the Preferred Reporting Items for Systematic Reviews and Meta-Analyses (PRISMA) statement. The primary goal was to evaluate SWE as a diagnostic tool for vulnerable carotid plaques.

Results: The search resulted in the identification of 606 studies, of which 24 specifically examined our primary objective. Five comparative studies were included in the symptomatic vs asymptomatic group of the meta-analysis, while three were included in the vulnerable vs stable group. Vulnerable and symptomatic carotid plaques showcased significantly lower Young's modulus (kPa) values (both, $p < .001$)

Conclusion: SWE has shown promising results for carotid plaque assessment and stroke risk stratification. Further prospective multicenter clinical studies are needed to determine optimal techniques and parameters for Young's modulus and shear wave velocity indexes, enhancing stroke prevention and treatment.

Keywords: elastography, ultrasound, carotid atherosclerosis, stroke

1. CAROTID DISEASE

1.1 Stroke burden

As reported by Global Burden of Disease (GBD) in 2019, stroke was the second most prevalent cause of mortality and the third most prevalent cause of disability globally. (1). This includes approximately 6.6 million deaths, loss of 143 million disability-adjusted life-years (DALYs), and 12.2 million new cases (1,2). The previous statement appears to be supported by the World Stroke Organization (3), as stroke remains the second-leading cause of mortality and the third-leading cause of disability and mortality combined on a global scale. The estimated global expenditure on stroke is more than US$721 billion, which is equivalent to 0.66% of total worldwide gross domestic product. Evidenced by a 70.0% increase in occurrence of cerebrovascular accidents, a 43.0% increase in stroke-related fatalities, a 102.0% surge in prevalent strokes, and a 143.0% rise in DALYs, the burden of stroke significantly increased between 1990 and 2019. The overwhelming majority of the worldwide stroke burden is concentrated in countries with lesser incomes (4,5). Annually in Europe, 1.4 million strokes occur in the 715 million Europeans and stroke is responsible for 1.1 million deaths. Also, an increasing number of Europeans are believed to be affected by stroke as a chronic disease; estimates place this figure at 4.6 million in 2035, up from 3.7 million in 2015 due to population aging (5,6). In 2015, European health systems allocated a total of €45 billion annually for stroke care, inclusive of indirect costs. Overall stroke expenses in the United States were €43.9 billion in 2015 and 2016, while by 2035 they are predicted to rise to € 114 billion (4–6).

1.2 Transient ischemic attack (TIA) and stroke definition

Stroke, as defined by the World Health Organization (WHO), is a condition that is characterized by the rapid development of clinical signs of focal or global neurological deficit. These signs can worsen and persist for 24 hours or more, potentially leading to death, and have no apparent cause other than vascular origin (7,8). In order to reclassify certain cases that were previously diagnosed as transient ischemic attacks (TIAs) as strokes, the WHO's definition has been expanded in the ICD-11 to include individuals with symptoms lasting less than 24 hours if neuroimaging reveals evidence of brain infarction. (9) Conversely, a TIA is defined as a brief episode of neurological dysfunction that is initiated by focal ischemia in the brain, spinal cord, or retina, without the presence of acute infarction (9). This

definition, which is tissue-based, emphasizes the absence of infarction, distinguishing it from the previous time-based definition, which focused on symptom resolution within 24 hours. TIAs are significant because they act as a warning for potential ischemic strokes, with a high risk of stroke occurring within 48 hours, notably following TIA (10,11). Early intervention is crucial in the management of TIAs, as it necessitates urgent assessment and treatment to prevent subsequent strokes. The redefinition of stroke and TIA by the WHO and the ICD-11 is indicative of a change in the understanding of cerebrovascular events, with the objective of enhancing the strategies for diagnosis, treatment, and prevention (8,9).

2. CAROTID ATHEROSCLEROSIS

2.1 Anatomy

The complex structure of the arterial wall layers and their physiological functions are crucial for a thorough understanding of the pathophysiological mechanisms involved in carotid stenosis. The carotid artery consists of three unique layers organized sequentially from inner to the outermost, namely the tunica intima, tunica media, and tunica adventitia. Each layer serves a distinct and important purpose, functioning as a non-thrombotic conduit that is crucial for sustaining cerebral blood flow, an essential process for ensuring optimal brain function and health. The carotid artery itself is inherently a highly flexible and adaptable structure, crucial for ensuring adequate blood flow to the corresponding cerebral hemisphere, thus facilitating the delivery of essential oxygen and nutrients to brain tissues (12). The tunica intima, the deepest and most metabolically active layer of the artery wall, mostly consists of endothelial cells essential for sustaining vascular homeostasis. This particular layer is essential for inhibiting platelet aggregation and preventing thrombus formation, therefore maintaining the general integrity of the vascular system. Adjacent to the tunica intima is the internal elastic lamina, consisting of a single layer of elastic fibers that confer structural support and elasticity to the artery wall. Adjacent to the internal elastic lamina lies the tunica media, acknowledged as the thickest layer of the arterial wall, distinguished by its intricate structure comprising a circumferential inner layer of smooth muscle cells (SMCs) and a longitudinal outer layer of SMCs, both embedded within a matrix abundant in proteins such as elastin and proteoglycans. The tunica media not only reinforces the arterial wall's structural integrity but also critically

modulates the vessel's diameter, regulating blood flow dynamics, vascular tone, and arterial pressure (12,13). The external elastic lamina covers the tunica medium, enhancing the artery's flexibility and distensibility. The outermost layer of the arterial wall is the tunica adventitia, mostly consisting of collagen fibers that provide strength and stability to the artery. This particular layer is acknowledged as the most resilient of the three and is essential in preventing undue dilation of the arterial wall under elevated blood pressure and flow, hence protecting the artery from potential damage and preserving its functional integrity. The stratified structure of arterial walls and their specific functions are crucial for preserving cerebrovascular health, underscoring the complex relationship between structure and function in the vascular system (12,13).

2.2 Mechanism

Atherosclerosis is defined not just as the abnormal accumulation of lipids but also as a continuous, complex inflammatory process. This process is characterized by significant alterations in wall shear stress (WSS) and low-density lipoprotein (LDL) infiltration (14). WSS refers to the circumferential pressure exerted by blood on the vessel's wall as it travels parallel to the direction of blood flow. In healthy settings, WSS promotes endothelial cell proliferation and inhibits the generation of inflammatory mediators and inflammation-related pathways (14–16). In the subintima, The buildup of lipids and foam cells disrupts the fluidity of the vessel wall, resulting in turbulent flow and subsequent alterations of WSS, which negatively impact endothelial cells, resulting in impaired function and compromised integrity of the tunica intima (17). In the initial phases of subintimal lipid accumulation and atheromatous material formation, adaptive vascular mechanisms prevent stenosis. The excessive growth of plaques caused by atherosclerosis exceeds the arteries' compensatory capacity, leading to alterations in hemodynamics of the vascular architecture (18). Plaque protrusion results in a decrease in lumen diameter, disrupting blood flow. Consequently, an area characterized by low WSS and increased oscillatory vascular stress is established, stimulating the ongoing atherosclerotic plaques formation (18,19).

2.3 Pathway

The onset and advancement of atherosclerosis are associated with reactive oxygen spe cies (ROS)(20,21). ROS enhance the production of cell adhesion molecules, including intercellular adhesion molecule-1, vascular cell adhesion molecule-1, and endothelial leukocyte adhesion molecule, which facilitate the attachment of monocytes to endothelial cells (22–24). Monocyte attachment to endothelial cells is facilitated by adhesion molecules. Low-density lipoprotein undergoes modest oxidation to form minimally modified LDL (MM-LDL), which prompts endothelial and SMCs to generate the chemoattractant protein-1 (MCP-1). The migration of monocytes to the subendothelial region, along with MCP-1, is facilitated by the further oxidation of MM-LDL, resulting in the formation of completely oxidized LDL (OX-LDL) (25–27).

OX-LDL functions as a ligand for the scavenger receptor in monocytes that has developed into tissue macrophages. The secretion of colony-stimulating factors, which is triggered by MM-LDL, promotes the differentiation of monocytes into macrophages. The differentiated macrophage acquires receptors for OX-LDL, which are incorporated to produce foam cells – which also produce ROS.

Macrophages produce a variety of growth-regulating molecules (e.g. platelet-derived growth factor - PDGF), and transforming growth factors (e.g. TGF-β), as well as cytokines that influence adjacent cells (28,29). The synthesis of elastic fiber proteins, collagen, growth-regulating molecules and cytokines may result from gene expression and transcription in SMCs. Growth-promoting molecules and cytokines are also synthesized by endothelial cells (29). T cells synthesize cytokines and TGF-β. SMCs also synthesize colony-stimulating factors which contribute to macrophage stability and proliferation. TGF-β is a powerful inducer of the creation of connective tissue and extracellular matrix components. It obstructs the reproduction of several cell types, along with SMCs. Cytokines stimulate the growth of SMCs. Both PDGF and IGF-I serve as chemoattractants for SMCs. Fibroblast growth factors serve as chemoattractants for endothelial cells, whereas M-CSF attracts monocyte-derived macrophages. (29)

In summary, atherosclerotic plaque formation is a complex pathophysiological process that begins with endothelial dysfunction, often triggered by conventional risk factors such as hypercholesterolemia, smoking, hypertension, and impaired glucose metabolism. This dysfunction increases endothelial permeability to lipoproteins,

facilitating the accumulation of LDL in the subendothelial space, where it undergoes oxidation. The OX-LDL functions as a chemoattractant, facilitating the attraction of monocytes and their development into macrophages. These macrophages engulf the OX-LDL to form foam cells, which are a characteristic of initial lesions of atherosclerosis identified as fatty streaks. Activated macrophages contribute to the chronic inflammatory environment within the plaque by releasing pro-inflammatory cytokines and matrix metalloproteinases, as well as the accumulation of foam cells. This inflammation is further exacerbated by T-cell activation and the release of additional cytokines, which perpetuate the inflammatory cycle and promote the migration and proliferation of SMCs from the media to the intima, establishing a fibrous cap over the lipid-rich core.

2.4 Vulnerable carotid plaque

Embolization risk from carotid plaques is highly variable. Some have reported a stroke risk of 0.5% per year in patients with high-grade stenosis, while others have demonstrated a risk of over 10% per year in patients with severe carotid stenosis.(30,31) Despite the fact that there were varying definitions of "high-grade" stenosis in the early clinical trials, most clinicians have now concurred that 70%–99% stenosis is classified as high-grade, according to the NASCET criteria (32). It is intriguing that the correlation between plaque vulnerability and the degree of stenosis remains uncertain. The development of cerebrovascular symptoms has not been demonstrated to be correlated with the degree of stenosis in numerous studies, including ACAS and ACST (33,34). The heterogeneity of carotid plaques is a significant factor in the variations in stroke risk. Not all carotid plaques exhibit identical behavior. Even at modest or moderate levels of stenosis, plaques that are referred to as "unstable" or "vulnerable" are found to be more susceptible to causing stroke or TIA (35). Silent, micro-infarcts have been observed in patients with carotid artery plaques that appear to be unstable (36,37). These plaques are referred to as "high-risk", while stable plaques are referred to as "quiescent." The "upstream" region, which is distal to the plaque, has been demonstrated to be particularly susceptible to shear stresses, which in turn leads to changes in stability (38,39). Plaque mobility has also been demonstrated to elevate the likelihood of microembolization and subsequent cerebral infarction (40,41).

Plaque stability can be assessed from a variety of perspectives, such as plaque content and morphology, plaque mobility, plaque hemodynamics, and surface characteristics. Plaque ulceration has been extensively investigated in terms of surface characteristics and has been consistently demonstrated to be associated with vulnerable plaque and microembolic activity (32,37,42). It has been demonstrated that ulcerated plaques frequently contain an element of overlying thrombosis and that the surface of ulcerated plaques exhibits an increase in platelet aggregation and activity (40,42,43).

Atherosclerotic plaques are typically composed of two primary components: a soft, lipid-rich portion and a firm, sclerotic portion that is primarily constituted of connective tissue elements. The calcified, connective tissue component has been suggested as a means of stabilizing the plaque. Consequently, plaques with a higher calcific component may be less susceptible to rupture (40,44). The inner atheromatous component of the lesion is thrombogenic and feeble, characterized by elevated macrophage activity and cellular detritus (45). Consequently, this results in intraplaque hemorrhage (IPH) and necrosis. Unstable plaque is characterized by a necrotic core and a high lipid content that are echolucent or hypoechoic on ultrasound (35,46). Plaque rupture risk has been associated with both the overall size of the plaque and the size of the necrotic interior (40,44,46).

The occurrence of plaque neovascularization (via angiogenesis) is a response to the escalating hypoxia within the interior of a plaque and has also been linked to instability. Soft, lipid-rich plaques demonstrate great increase in neovascularization in comparison to soft, calcified plaques (47–49). Neovascularization has been associated with IPH since immature neo-vessels can bleed and consequently lead to thrombosis and acute plaque enlargement (50,51).

Still, it is believed that plaques with larger dimensions (area or volume) are associated with a greater degree of stenosis. The risk of plaque rupture is heightened by both the necrotic core size and the overall plaque size. It is noteworthy that there is no definitive correlation between the vulnerability of plaques and the degree of stenosis, as the treatment algorithms between patients with unstable and stable plaques may ultimately differ.

3. CLASSIFICATIONS OF CAROTID ATHEROSCLEROTIC PLAQUE

3.1 B-mode (Echolucency)

Gray-Wale (52) is the original classification of carotid atherosclerotic plaques depending on their echolucency. In 1993 Geroulakos et al. (53) modified the original Gray-Wale classification (52) and classified carotid plaques as follows, adding a fifth category *Table 1*.

Type I	Uniformly echolucent plaques.
Type II	Predominantly echolucent plaques with < 50 per cent echogenic areas
Type III	Predominantly echogenic plaques with < 50 per cent echolucent areas
Type IV	Uniformly echogenic plaques
Type V	Plaques that could not be classified owing to heavy calcification and acoustic shadows.

Table 1 – Geroulakos et al. modified Gray-Weale Classification

3.2 American Heart Association (AHA) Classification

The AHA classification (54) (*Table 2)* categorizes atherosclerotic carotid plaques into types I-VIII based on histopathological features. These range from early lesions (types I/II) to advanced lesions with complications such as hemorrhage or thrombosis (type VI) and calcified plaques (type VII). The MRI-modified adaptation (55) uses MRI to assess plaque vulnerability, correlating dynamic contrast-enhanced MRI parameters with plaque types.

Original AHA Classification (56)	**Modified AHA Classification** (57)
Type I: initial lesion with foam cells	Type I-II: near-normal wall thickness, no calcification
Type II: fatty streak with multiple foam cell layers	
Type III: preatheroma with extracellular lipid pools	Type III: diffuse intimal thickening or small eccentric plaque with no calcification
Type IV: atheroma with a confluent extracellular lipid core	Type IV–V: plaque with a lipid or necrotic core surrounded by fibrous tissue with possible calcification
Type V: fibroatheroma	
Type VI: complex plaque with possible surface defect, hemorrhage, or thrombus	Type VI: complex plaque with possible surface defect, hemorrhage, or thrombus
Type VII: calcified plaque	Type VII: calcified plaque
Type VIII: fibrotic plaque without lipid core	Type VIII: fibrotic plaque without lipid core and with possible small calcifications

Table 2 – AHA Classifications

4. ELASTOGRAPHY

Elastography, first introduced in the 1990s, (56,57) facilitates the assessment of the elastic characteristics of vascular tissues and has extensive applications in the examination of physiology and pathology of arteries. This method depends on observing deformation of tissue caused by stimuli, internal or external. Through the process of inverse analysis one can derive and interpret the mechanical characteristics of soft tissues, based on the specific responses that are recorded during the application of such stimuli. As presented in *Table 3* strain and shear wave elastography (SWE) are techniques used to evaluate tissue mechanical characteristics by estimating strain and shear wave velocity (or Young's Modulus), respectively.

4.1 Strain elastography

When a practitioner applies force to a tissue using a probe oriented in alignment with the trajectory of the ultrasound beam, deformation of the tissue ensues. The rate of strain (deformation) can be evaluated through the analysis of the echo signal both prior to and during the compression phase. Young's modulus (YM) is used to quantify the stiffness of tissue and is calculated using the equation ($E = s/\varepsilon$) subsequent to the application of stress – s, and the acquisition of strain measurement - ε. Given the challenges associated with ascertaining the internal stress distribution within the body, it is typically assumed to be uniform. As a result, strain exhibits an inverse relationship with stiffness. The strain representation is overlaid as a color gradient on the B-mode image. Numerous ultrasonic devices also display elastograms that are gray and other color-coded variants. A real-time quality indicator is provided to indicate whether the applied compression is appropriate. Strain functions as a relative indicator of stiffness and exhibits a proportional variation in response to the level of compression applied (58–60).

Strain elastography is significantly operator-dependent, as it necessitates manual compression to generate strain, which may vary among operators and impact the consistency of results. In addition, it offers a qualitative evaluation of tissue rigidity, which may result in results that are inconsistent due to operator dependence and the subjective nature of the interpretation(61,62).

4.2 Shear wave elastography

The various techniques employed in the assessment of SWE can be distinctly classified into two primary categories, namely, the techniques predicated upon transient elastography as well as those utilizing Acoustic Radiation Force Impulse (ARFI), which fundamentally differ in their particular excitation methods, as it is subsequently described (63).

4.2.1 Transient Elastography

An ultrasonic transducer is integrated with a mechanical piston, facilitating manual manipulation to produce thrust on the surface of the body. This thrust applies force to the liver through the intercostal space, leading to transient shear deformation and the transmission of shear waves. Shear wave velocity (SWV) propagation is directly correlated with the stiffness of the liver parenchyma; increased stiffness results in faster propagation. Currently, this methodology is exclusively employed for assessing liver stiffness (58).

4.2.2 ARFI based SWE techniques

The methodologies of ARFI differ from those of transient elastography in their application of mechanical stimulation. Specifically, an acoustic radiation force induces tissue displacement and shear wave propagation through a focused acoustic beam (63). Shear waves travel perpendicularly to the ultrasonic waves; hence, shear wave velocity (SWV) is determined by observing the time to peak displacement at each lateral point. Tissue oscillations within a region of interest (ROI) facilitate the production of shear waves via frequency-specific push pulses, which exhibit a prolonged duration and elevated intensity compared to those employed in traditional B-mode imaging. The recorded velocity is positively correlated with an increase in frequency. B-mode imaging guidance remains viable throughout the assessment, as both techniques utilize the same transducer (58,63). The YM ($E = 3\rho Vs2$), where, ρ for tissue density, and Vs for SWV can be used to convert this velocity to tissue stiffness measured in kilopascals (kPa) under specific assumptions (64). The real-time tracking of shear wave propagation was not achievable in ARFI-based SWE due to its lack of reliance on ultrafast imaging rates. Rather, it was reconstructed in a stroboscopic fashion through the application of multiple successive radiation force impulses combined with various imaging lines. This repeated application of radiation forces resulted in a greater deposition of acoustic energy, which consequently limited

the frame rate and functional capabilities of ARFI-based SWE for real-time elasticity assessment (58,60,63). Three subcategories of ARFI based SWE are addressed below depending on the extend of the observed region:

Point shear wave elastography

Point shear wave elastography (p-SWE) exclusively triggers the acoustic radiation force at a specific location and subsequently quantifies the shear wave velocity within a confined ROI. The results are expressed in either meters per second (m/s) or kPa, as dictated by the YM equation. Given the restricted area evaluated in shear wave imaging, it is recommended to perform a minimum of 5 to 10 measurements and compute the mean value (65).

Two-dimensional shear wave elastography

Through the continuous activation of the acoustic radiation force at multiple locations and the subsequent assessment of the shear wave's arrival time utilizing a time-of-flight estimation methodology, it is feasible to produce a shear wave image of an expanded area of interest, which can be represented in either grayscale or color scale (58,66). This type of shear wave imagery can be displayed autonomously or superimposed onto the conventional B-mode visualization. A measurement box can be placed within the ROI to ascertain the stiffness value The measurement box should preferably be situated in the central area of the ROI, as inaccuracies frequently arise near the peripheries. In contrast to p-SWE, the dimensions of the measurement box in two-dimensional shear wave elastography (2D-SWE) can be modified, and 2D-SWE offers not only the mean and the standard deviation of stiffness assessments but also the minimum and maximum values. If the system includes a quality metric that indicates the measurement area produces high-quality shear waves, it is recommended to perform three to five measurements (58,66,67).

Three-dimensional shear wave elastography

A three-dimensional probe is essential for the implementation of three-dimensional shear wave elastography (3D-SWE). This probe integrates a mechanical scanning sequence utilizing two-dimensional sensors and possesses advanced computational capabilities, thus facilitating the three-dimensional reconstruction of tissue stiffness.

The application of 3D-SWE for the assessment of plaque vulnerability remains to be explored (58).

Technique	Measurement	Stimulation	Method	Indicator
Strain imaging	Strain	Manual Compression	Strain Elastography	Elasticity score Strain ratio E/B size ratio
Shear wave imaging	Shear wave velocity	Mechanical Vibration		Young's Modulus (kPa) Shear wave velocity (m/s)
		ARFI	p-SWE	Young's Modulus (kPa) Shear wave velocity (m/s)
			2D-SWE	Young's Modulus (kPa) Shear wave velocity (m/s)
			3D-SWE	Young's Modulus (kPa) Shear wave velocity (m/s)

Table 3 – Types of Elastography

5. SYSTEMATIC REVIEW AND META-ANALYSIS

The role of shear wave elastography in the assessment of carotid plaque vulnerability – A Systematic Review and Meta-analysis

5.1 Introduction

Cerebrovascular events are usually triggered by the rupture of carotid atherosclerotic plaques. The etiology of up to 80% of strokes is ischemic, with cerebral micro-embolism accounting for 10% to 20% (1,68).

Stroke is the second leading cause of death and disability globally, with 12.2 million incidents, 143 million lost disability-adjusted life-years, and 6.6 million deaths in 2019 (1). The cost of stroke exceeds $721 billion, constituting 0.66% of global GDP. Between 1990 and 2019, the burden of stroke increased significantly, with the majority in lower-income countries (4,5). Early intervention is crucial in managing stroke and transient ischemic attacks (TIAs), preventing subsequent strokes.

The correlation between plaque vulnerability and the degree of stenosis remains uncertain, as the development of cerebrovascular symptoms has not been demonstrated to be correlated with just the degree of stenosis in numerous studies (33,34). The heterogeneity of carotid plaques is a significant factor in the variations in stroke risk. The heterogeneity of carotid plaques constitutes a critical determinant in the disparities observed in stroke risk. Even at modest or moderate degrees of stenosis, lesions characterized as unstable or vulnerable are observed to possess a heightened propensity for precipitating stroke or transient ischemic attack (TIA)(35). Silent micro-infarcts have been identified in patients exhibiting unstable carotid artery. These plaques are referred to as "high-risk", while stable plaques are referred to as "quiescent" (37,38). Plaque stability can be evaluated from multiple dimensions, including plaque composition and morphology, plaque mobility, hemodynamic properties, and surface characteristics. The ulceration of plaques has been the subject of extensive research concerning their surface characteristics, and it has been consistently shown to correlate with vulnerable plaques and microembolic activity(37,42).

Atherosclerotic plaques are generally comprised of two principal components: a flexible, lipid-rich segment and a dense, sclerotic segment predominantly made up of connective tissue elements (40). The likelihood of plaque rupture has been correlated with both the overall dimensions of the plaque and the extent of the necrotic core (45).

Intraplaque hemorrhage (IPH) and neovascularization, which occurs as a response to increasing ischemia within the core of a plaque, has also been associated with instability (50,51).

Elastography, a technique that emerged in the 1990s (56,57), is employed to evaluate the elastic properties of vascular tissues and has a wide range of applications in the study of arterial physiology and pathology. It is predicated on the observation of tissue deformation resulting from external or internal stimuli, and the mechanical properties of soft tissue can be inferred from the observed responses through inverse analysis. Strain elastography and shear wave elastography are sophisticated techniques utilized to assess the mechanical properties of tissues by measuring strain and shear wave velocity (or shear modulus), respectively. Strain elastography (59,63) entails the examination of the echo signal both prior to and during the application of compression, whereas shear wave elastography measures tissue stiffness in terms of Young's modulus. Shear wave-based elastography (63) can be classified into two categories: transient elastography and Acoustic Radiation Force Impulse (ARFI) based SWE, contingent upon the method of excitation employed. Transient elastography (58) has not yet been employed for the evaluation of arterial rigidity or the assessment of plaque vulnerability. ARFI-based shear wave elastography employs mechanical stimulation to induce tissue displacement and generate shear waves. The velocities of these shear waves can be determined by measuring the time taken to reach maximal displacement at each lateral point (58,60). This approach has shown efficacy in distinguishing between stable and susceptible plaques, which is crucial for clinical decision-making about procedures such as carotid endarterectomy or stenting (69,70).

Overall, strain and SWE serves as an essential instrument for the non-invasive evaluation of carotid plaque vulnerability, potentially influencing treatment choices and enhancing patient outcomes in carotid artery disease (71).

5.2 Scope

The scope of this study is to examine the role of SWE on imaging the carotid plaque by systematically reviewing the available literature on SWE assessing the vulnerability of the carotid plaque and its potential role on predicting carotid stenosis related symptoms. A meta-analysis of the available data was conducted.

5.3 Methodology

A systematic review and meta-analysis were conducted to review the use of shear wave elastography for the evaluation of the atherosclerotic carotid plaque and study its ability to assess the vulnerability of the plaque. The approach of the present work was based on the Preferred Reporting Items for Systematic Reviews and Meta-Analyses (PRISMA) statement (72).

5.3.1 Databases and search terms

The studies were identified through a comprehensive search of electronic databases and by reviewing the bibliographic references of relevant articles. A search was run in the National Library of Medicine's MEDLINE database using the PubMed interface, Cochrane library and Scopus and ClinicalTrials.gov. There were no language constraints on the first screening. The most recent search was conducted on July 14, 2024. Keywords were chosen utilizing medical subject headings (MeSH) for PubMed and Cochrane and MeSH/Emtree for Scopus. The keywords “carotid”, “elastography” and “shear wave” were combined. The databases were searched with an unrestricted search strategy, applying exploded MeSH and keywords combined with the Boolean operators “AND” or “OR” to retrieve relevant reports, as reported in the search strategy *Table 4.*

	Search strategy	**Results**
MEDLINE (PubMed)		
1	"carotid arteries"[MeSH Terms] OR ("carotid"[All Fields] AND "arteries"[All Fields]) OR "carotid arteries"[All Fields] OR "carotid"[All Fields] OR "carotids"[All Fields] OR "carotidal"[All Fields] OR "carotide"[All Fields] OR "carotideal"[All Fields]	159,768
2	"elasticity imaging techniques"[MeSH Terms] OR ("elasticity"[All Fields] AND "imaging"[All Fields] AND "techniques"[All Fields]) OR "elasticity imaging techniques"[All Fields] OR "elastographies"[All Fields] OR "elastography"[All Fields] OR "SWE"[All Fields] OR (("shear"[All Fields] OR "sheared"[All Fields] OR "shearing"[All Fields] OR "shearings"[All Fields] OR "shears"[All Fields]) AND "wave"[All Fields])	23,835
3	#1 AND #2	**404**
SCOPUS		

1	TITLE-ABS-KEY: carotid	42,129
2	TITLE-ABS-KEY: elastography OR SWE OR shear wave	19,515
3	#1 AND #2	**95**
Cochrane Library		
1	All Text: (elastography OR SWE OR shear wave)	2030
2	All Text: carotid	10351
3	#1 AND #2	**47**
ClinicalTrials.gov		
1	Disease: Carotid	1017
2	Other: Elasticity Imaging Techniques OR Shear Wave Imaging	1537
3	#1 AND #2	22

Table 4 – Search strategy

5.3.2 Study selection

Zotero software (Corporation for Digital Scholarship, Center for History and New Media at George Mason University, USA) was employed to gather the studies identified in all database searches. Duplicates were removed using Zotero software. No search was conducted to retrieve any unpublished data or abstracts. Eligibility assessment was performed independently in an unblinded standardized manner by two authors (CP and SK). Any discrepancies in the inclusion of studies were resolved through consensus.

5.3.3 Inclusion and exclusion criteria

All human studies concerning strain or shear wave elastography for the assessment of the carotid plaque vulnerability were eligible for review. Non-English articles, in vitro, animal, phantom and simulation studies, editorials, letters to the editor and abstracts were excluded. Reviews were also excluded to avoid duplication of data. Articles that did not sufficiently report data, were excluded. Also excluded were the studies on elastography that did not examine its use on carotid plaque (e.g. other

organs/sites, solely arterial stifness) or strain elastography. For homogenisation purposes and robust statistical results, mean and standard deviation values were the sole metrics obtained. during the search.

5.3.4 Quality Assessment

The methodological quality of each study was assessed independently by two authors (CP and SK) with the revised Quality Assessment of Diagnostic Accuracy Studies (QUADAS-2) tool (25). This tool comprises four domains: (1) patient selection; (2) index text; (3) reference standard; and (4) flow and timing as presented in. These four domains were assessed regarding risk of bias and the first three in terms of concerns regarding applicability. Possible answers for risk of bias for the different domains were high, low, some concerns or no information. The quality assessment is visually presented in *Figure 1* and *Figure 2*.

5.3.5 Data Pooling

Due to the heterogeneity of the reported carotid plaque stiffness data, provided sample size, median, range and/or interquartile range or other convertible data (e.g. Confidence Interval) were converted to mean ± standard deviation utilizing the appropriate estimation methods as suggested by Wan et al. (73) and in accordance to the Cochrane handbook (74). Studies providing insufficient or unconvertable data were excluded. Data were extracted and entered into tables and the outcomes were analyzed cumulatively.

Figure 1- Risk cf bias visualization

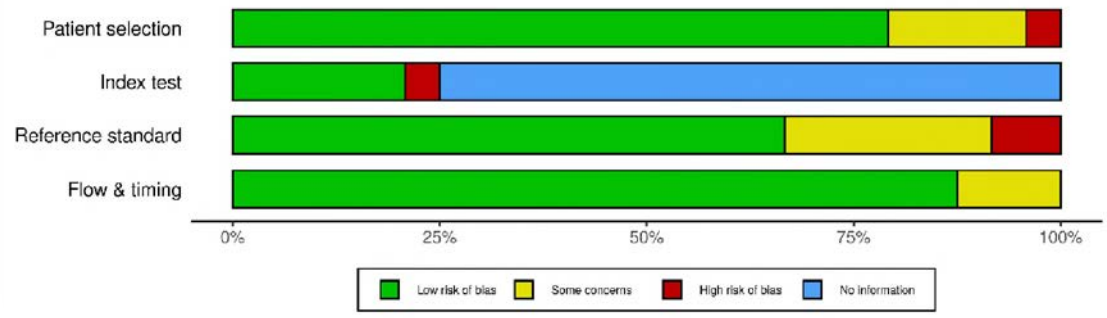

Figure 2 – Risk cf bias summary graph

5.3.6 Meta-analysis

Standardized mean difference (SMD) and 95% CIs were estimated for the continuous outcomes. SMD < 0 indicated lower values in the Symptomatic or Vulnerable plaque group. Between-study heterogeneity was assessed through Cochran Q statistic and by estimating I^2. I^2 greater than 50% and $p<.01$ indicated significant heterogeneity. Due to the significant between-study clinical heterogeneity, we used the random-effects model (DerSimonian–Laird) (75) to calculate the pooled effect estimates for all outcomes. A forest plot for each outcome was used to display the pooled estimates graphically. Statistical significance was set at 0.05, and all *p*-values were two-tailed.

5.4 Results

The search, by following the aforementioned methodology, resulted in the identification of 606 studies, of which 24 (*Table 5)* specifically examined our primary objective of assessing the feasibility of shear wave elastography (SWE) in the risk stratification of carotid plaque. These studies were subsequently included in the systematic review as presented in *Figure 3*.

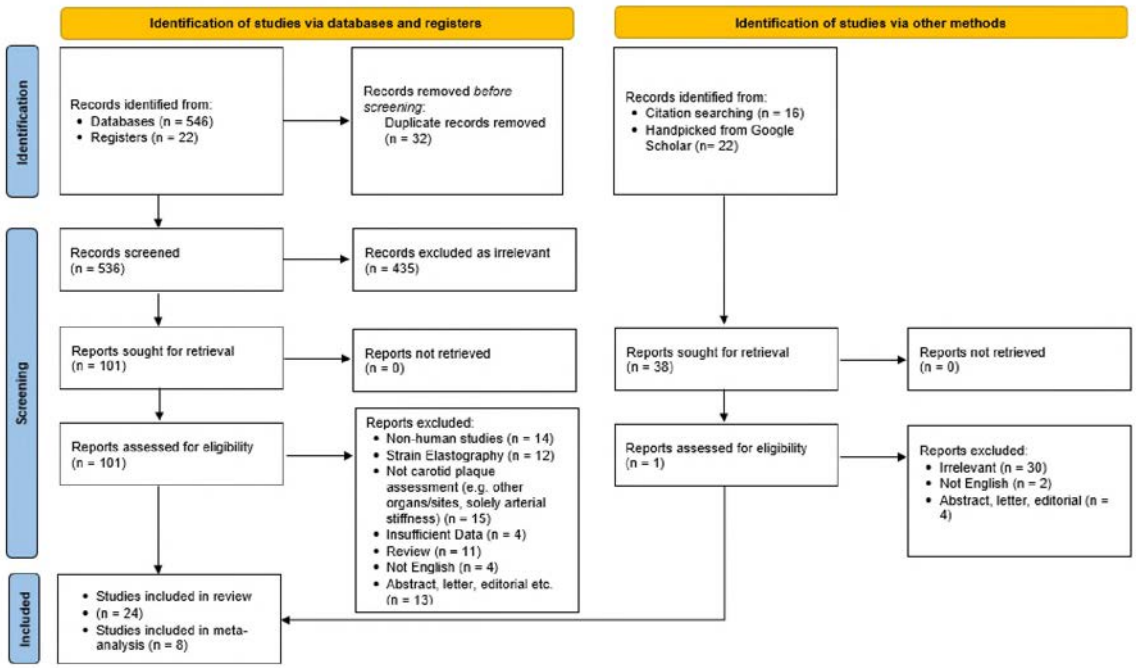

Figure 3 – PRISMA flow chart

Author (Year)	Sample size (stable; asymptomatic / unstable; symptomatic)	SWE type	Device	Probe (Frequency)	Reference method	Elasticity (kPa)		Outcomes
						Stable / Asymptomatic	Vulnerable / Symptomatic	
Dahl et al. (2009)	23	ARFI	Siemens Antares™ (Siemens Medical Solutions USA, Inc., Issaquah, WA, USA)	Linear array probe (5-10 MHz)	B-mode	N/A	N/A	ARFI imaging was shown to be an effective, non-invasive technique for observing the mechanical makeup of carotid plaques.
Ramnarine et al. (2014)	47 (20/27), 54 plaques	SWE	Aixplorer® ultrafast ultrasound system scanner with (Supersonic Imagine, Aix-en-Provence, France)	Linear array probe (4-15 MHz)	• Neurological symptoms • Histology	mean 62; 95% CI = 51 – 73	mean 88; 95% CI = 71 105	The mean plaque YM of the symptomatic patients was significantly lower (p = 0.01) than the mean plaque YM of the asymptomatic patients
Doherty et al. (2015)	5	ARFI	Acuson S2000 (Siemens Healthcare, Erlangen, Germany)	Linear array probe (4-9 MHz)	B-mode	N/A	N/A	ARFI imaging displacements may provide important prognostic information related to plaque vulnerability.

Garrard et al. (2015)	25 (16/9)	SWE	Aixplorer® ultrafast ultrasound system scanner with (Supersonic Imagine, Aix-en-Provence, France)	Linear array probe (4-15 MHz)	Histology	79 ± 33.8 (mean ± SD)	50 ± 19.6 (mean ± SD)	• The mean plaque YM of the vulnerable plaques was significantly lower (p = 0.027) than the mean plaque YM of the stable plaques • The presence of plaque hemorrhage, thrombus and increasing numbers of foam cells was also associated with a significantly lower YM
Lei et al. (2016)	199	SWE	Aixplorer® ultrafast ultrasound system scanner with (Supersonic Imagine, Aix-en-Provence, France)	Linear array probe (2-10 MHz)	B-mode	N/A	N/A	SWE is a noninvasive, reproducible and reliable imaging technique which could be as an addition of early detection of vulnerable plaques in the carotid artery.
Czernuszewicz et al. (2017)	25	ARFI	Siemens Acuson Antares (Siemens Medical Solutions USA Inc., Ultrasound Division)	Linear array probe (3-7 MHz)	Histology	N/A	N/A	Good performance for combined ARFI and stiff (median AUC: 0.859) and soft (0.887) categories.
Lou et al. (2017)	61 (30/31)	SWE	Aixplorer® ultrafast ultrasound system scanner with (Supersonic	Linear array probe (2-10 MHz)	• B-mode (GSM) • Symptomatology	115.78 ± 26.66 (mean ± SD)	81.13 ± 20.12 (mean ± SD)	The mean YM of the representative plaques in symptomatic group was significantly lower than

			Imagine, Aix-en-Provence, France)					that in asymptomatic group ($p < .01$)
Di Leo et al. (2018)	43 (12/31)	SWE	Aplio 500 (Toshiba Medical Systems Corporation Otawara, Japan)	Linear array probe (5-14 MHz)	Histology	N/A	N/A	• High diagnostic accuracy of SWE in identifying vulnerable plaques • Results show that SWE sensitivity 87.1% is comparable to CTA (87.1%); nevertheless, SWE has higher number of false positive cases, which leads to a lower specificity 66.7% in comparison to CTA (100%).
Shang et al. (2018)	129 (44/85)	SSI	Aixplorer® ultrafast ultrasound system scanner with (Supersonic Imagine, Aix-en-Provence, France)	Linear array probe (4-15 MHz)	• Echolucency • Serum homocysteine levels • Neurological Symptoms	N/A	N/A	• Echogenic plaques had higher SWVs than echolucent ones (SWVmin, 3.91 [3.24−4.17] m/s vs. 1.51 [1.04−1.94] m/s; SWVmean, 4.29 [3.98−4.57] m/s vs. 2.09 [1.69−2.41] m/s; SWVmax, 4.67 [4.33−4.86] m/s vs. 2.62 [2.32−3.31] m/s; all p values < 0.01) • Serum homocysteine levels were negatively correlated with SWVmin ($r = -0.205$, $p = 0.020$), SWVmean ($r = -0.213$, $p = 0.015$), and SWVmax ($r = -0.199$, $p = 0.024$).
Sivasankar et	60 (30/30)	SWE	Acuson S3000 (Siemens	Linear array probe (4-9 MHz)	Neurological Symptoms	Proximal: mean 37.87	Proximal: mean 26	The proximal, mid, and distal stiffness values of the

al. (2019)			Healthcare, Erlangen, Germany)			Mid: mean 42.67 Distal: mean 43.97	Mid: mean 24.05 Distal: mean 24.01	plaque were less on the side on which the stroke had occurred as compared to the non-stroke side with a statistically significant difference ($P < 0.05$).
Torres et al. (2019)	25	ARFI	Siemens Acuson Antares (Siemens Medical Solutions USA Inc., Ultrasound Division)	Linear array probe (3-7 MHz)	Histology	N/A	N/A	By incorporating both correlation coefficient (CC) and signal-to-noise ratio (SNR) into a single metric, log(VoA) parameter significantly improves the delineation of carotid atherosclerotic plaque features compared to ARFI peak displacement (PD)
Marlevi et al. (2020)	27		General Electric Logiq E9 system (GE Healthcare, Wauwatosa, WI, USA)	Linear array probe (9 MHz)	MRI (AHA)	N/A	N/A	Significantly higher SWV in AHA type VI plaques.
Zhang et al. (2021)	94 Symptomatic patients, 98 plaques	SWE	Acuson HELX3000, (Siemens Healthcare,Erlangen,Germany)	Linear array probe (4-9 MHz)	Histology	N/A	N/A	• There was a negative correlation between the SWV of SWE and plaque neovascularization. ($p < .001$) • The SWV of SWE was significantly positively correlated with the type I/III collagen ratio ($p < .001$)

Yi Li et al. (2021)	123 (58/65)	SWE	Aplio 900 (Canon Medical Systems Corporation, Japan)	Linear array probe (5-14 MHz)	Neurological Symptoms	78.5 ± 25.4 (mean ± SD)	51.5 ± 18.3 (mean ± SD)	• The mean plaque YM of the symptomatic patients was significantly lower ($p < .001$) than the mean plaque YM of the asymptomatic patients. • Combining the YM with IPN grades yielded improved discrimination performance (AUC =0.89).
Skoloudik et al. (2021)	97 patients with >50% carotid stenosis (74 stable asymptomatic/12 progressive asymptomatic/11 symptomatic	SWE	Aixplorer® ultrafast ultrasound system scanner with (Supersonic Imagine, Aix-en-Provence, France)	Linear array probe (4-15 MHz)	Neurological Symptoms	Stable: 52.2 ± 30.0 (mean ± SD) Progressive: 30.4 ± 17.9 (mean ± SD)	64.5 ± 10.2 (mean ± SD)	• The mean elasticity measured using the YM was significantly higher in asymptomatic stable plaques compared with asymptomatic progressive and symptomatic plaques. • No significant difference in elasticity was found between asymptomatic progressive and symptomatic plaques
Carter et al. (2022)	41	pSWE	Mindray Resona 7 Ultrasound system (Mindray Bio-Medical Electronics Co., Ltd., Shenzhen,	Linear array probe (3-9 MHz)	B-mode	N/A	N/A	SWE data as an additional means of characterizing focal atheromata during routine carotid sonographic examinations is feasible and

			China)					reliable
Goudot et al. (2022)	46 (17/29)	SWE	Aixplorer® ultrafast ultrasound system scanner with (Supersonic Imagine, Aix-en-Provence, France)	Linear array probe (2-10 MHz)	Histology	N/A	N/A	• Mean plaque stiffness of 3.6 ± 1.4 m/s for vulnerable plaques and 3.0 ± 1.4 m/s for stable plaques. • No significant difference between symptomatic and asymptomatic patients (mean 3.52 ± 1.36 Vs 3.60 ± 1.40 m/s)
Mazzacaro et al. (2023)	63 (30/33)	pSWE	Esaote MyLab ultrasound system (EsaoteTM, Genova, Italy)	Linear array probe (7.5 MHz)	Histology	49.6 ± 8.1 (mean ± SD)	24.6 ± 4.3 (mean ± SD)	• YM was found to be significantly higher in patients with stable plaques (49.6 ± 8.1 kPa vs. 24.6 ± 4.3 kPa, p = 0.009). • For the measurement of YM, values >34 kPa had a sensitivity of 50% and a specificity of 73.3% in predicting plaque non-vulnerability (accuracy = 62.9%, AUC = 0.66 ± 0.03)
Wang et al. (2023)	244 (176/68)	SWE	Aixplorer® ultrafast ultrasound system scanner with (Supersonic Imagine, Aix-en-Provence, France)	Linear array probe (2-10 MHz)	CEUS	Max: 39 (20) Mean: 27.40 (22.1) Min: 18.10 (17.0)	Max: 25 (10.5) Mean: 21 (15.8) Min: 10.80 (15.5)	• A positive correlation was found between plaque echotype, GSM and YM (P = 0.000), that the lower the GSM, the lower the echo and the lower the hardness value. • AUC of echotype was the lowest, and the sensitivity and specificity were also significantly lower than

								those of other methods, with statistically significant differences (P<0.001).
Zhang et al. (2023)	(38/62)	SWE	General Electric Logiq E9 system (GE Healthcare, Wauwatosa, WI, USA)	N/A	MRI (AHA)	N/A	N/A	Considering the final clinical diagnosis as the gold standard, the sensitivity, specificity, PPV, and NPV of SWE in assessing carotid artery vulnerability were 87.10% (54/62), 76.32% (29/38), 85.71% (54/63), and 78.38% (29/37), respectively. These results were in agreement with the final clinical results (Kappa = 0.637, P < 0.05)
Chen et al. (2024)	244 (Sympto matic Vs Control)	SWE	Aixplorer® ultrafast ultrasound system scanner with (Supersonic Imagine, Aix-en-Provence, France)	Linear array probe (2-10 MHz)	Neurological Symptoms	18.4 ± 10.6 (mean ± SD)	13 ± 8.8 (mean ± SD)	The risk of stroke was significantly associated with IPN (OR =3.93; 95% CI: 1.236.58; P=0.034) and SWV (OR =0.39; 95% CI: 0.16-0.98; P=0.045).
Globa et al. (2024)	96 (45/51)	SWE	Aplio 400 (Toshiba Medical Systems Corporation Otawara, Japan)	N/A	Neurological Symptoms	N/A	N/A	Microvascularization low stiffness can characterize the potential instability of the plaque. These criteria should be added to the traditional US assessment of carotid plaques.
Popov a et al.	24	2D-SWE	Esaote MylabX8 device (Esaote Esaote S.p.A.-sole-	Linear array probe (4-15 MHz), on 10Hz	B-mode	N/A	N/A	The optimal cut-off value of 2D-SWE > 32.40 kPa was associated with a sensitivity

(2024)			shareholder company Via Enrico Melen 77, 16152 Genova, Italy)					of 96%, a specificity of 56%, a PPV of 66.70%, and a NPV of 92.90%
Zhang et al. (2024)	121	SWE	EPIQ Elite scanner (Phillips, Amsterdam, the Netherlands)	Linear array probe (3-12 MHz) and (3-14MHz)	B-mode	N/A	N/A	The risk of stroke was significantly associated with IPN (OR =3.93; 95% CI: 1.236.58; P=0.034) and SWV (OR =0.39; 95% CI: 0.16-0.98; P=0.045)
N/A = Not applicable, GSM = Gray scale median, YM = Young's modulud SWE = Shear wave elastography, pSWE = point SWE, 2D-SWE = Two-dimensional SWE, ARFI = Acoustic radiation force impulse, SWV = Shear wave velocity, AHA = American Heart Association, MRI = Magnetic resonance imaging, CTA = Computed tomography angiography, CEUS = Contrast enhanced ultrasound, AUC = Area under curve, PPV = Positive prognostic value, NPV = Negative prognostic value								

Table 5 – Characteristics of studies included in review

As the need for new non-invasive techniques for carotid plaque vulnerability assessment emerged Dahl et al. (76), in 2009, studied the feasibility of ARFI in assessing the carotid plaque vulnerability. In this first in vivo feasibility study B-mode images were acquired immediately before each ARFI image to provide complementary data and as reference. ARFI imaging was identified as a feasible technique for noninvasively observing and characterizing the mechanical composition of carotid plaques, potentially assisting in the evaluation of ischemic event risk. This preliminary study offers important information for future studies regarding plaque characterization and the clinical applications of SWE/ARFI imaging.

5.4.1 Symptomatic Vs Asymptomatic plaques

In 2014, Ramnarine et al. (77) were the pioneers in categorizing subjects based on their history of neurological symptoms associated with carotid atherosclerotic disease and consequently compare their elasticity values. They found that plaques associated with focal neurological symptoms had significantly lower mean YM compared to asymptomatic plaques (62 kPa vs. 88 kPa; p =.01). Also, a significant correlation was reported between plaque YM and percentage of stenosis (p=.003), while when the two methods were combined the diagnostic accuracy was enhanced with an AUC of 0.78. Following these findings Lou et al. (78) also found significantly lower (p <.01) YM in the asymptomatic group (81.13 ± 20.12 kPa) versus symptomatic (115.78 ± 26.66 kPa), coming to accordance with a 2021 study (79) that found statistically significant (p <.001) difference of the mean elasticity values, reporting 78.1±25.4 kPa for asymptomatic and 51.5±18.3 kPa for symptomatic plaques.

In an observational, prospective pilot study Sivasankar et al. (80) measured the elasticity of stroke and non-stroke side, while separating the plaque to proximal mid and distal parts. All stiffness values were significantly lower (p <.05) on the stroke side. Also, all stiffness values of the plaque were significantly higher (p<.05) on the left compared to the right.

Skoloudik et al. (81) attempted to differentiate between asymptomatic stable, progressive and symptomatic plaques. The mean elasticity in the asymptomatic stable plaque group was significantly higher than in the asymptomatic progressive (52.2 vs. 30.4 kPa; p < 0.001) and symptomatic (52.2 vs. 36.4 kPa; p = 0.033) plaque groups. They reported an AUC of 0.70 for differentiating stable asymptomatic plaques from

progressive or symptomatic plaques and that sensitivity and specificity for a cut-off value of 26 kPa were 83.6% and 40.0%, respectively. They also surprisingly found that asymptomatic stable, asymptomatic progressive and symptomatic plaques did not differ in echogenicity, calcifications, homogeneity, occurrence of ulcerated surface, or intra-plaque hemorrhage ($p > .05$ in all cases).

Most recently, Globa and Derkach (82) found that the stiffness of plaques, as measured by SWE, was significantly lower in patients with ischemic events compared to those with asymptomatic stenosis ($p < .001$). Specifically, the median YM was 70.0 kPa (IQR: 57.0-80.0 kPa) in the right ICA and 72.0 kPa (IQR: 60.0-79.0 kPa) in the left ICA for the symptomatic group. In contrast, the asymptomatic group had a median YM of 82.0 kPa (IQR: 77.5-89.0 kPa) in the right ICA and 85.0 kPa (IQR: 74.0-94.0 kPa) in the left ICA. Adding to these Chen et al. (83) highlighted that the risk of stroke was significantly associated with SWV ($p = .045$).

5.4.2 Vulnerable Vs Stable plaques

In a 2015 novel prospective observational comparative study of 25 carotid plaques, Garrard et al. (84) reported that the mean plaque YM (50.0 ± 19.6 kPa) of the vulnerable plaques was significantly lower ($p = .027$) than the mean plaque YM (79.1 ± 33.8 kPa) of the stable plaques. Plaque stability was based on histology.

Di Leo et al. (85) exploring the diagnostic accuracy of SWE reported a sensitivity of 87.1%, a specificity of 66.7%, a positive predictive value of 87.1% and a negative predictive value of 66.7% for detecting vulnerable plaques. These findings came to accordance with a recent study by Zhang et al. (86) who underlined that SWE results were generally consistent with the final clinical diagnosis, showing a sensitivity of 87.10%, specificity of 76.32%, positive predictive value of 85.71%, and negative predictive value of 78.38% reaffirming SWE as a useful tool for assessing carotid plaque vulnerability.

In a prospective observational study by Goudot et al. (87) plaque stiffness measured by SWV did not differ between vulnerable and stable plaques, while for the range of 3–5 m/s SWV was significantly increased in vulnerable plaques ($p = 0.048$). They alternatively proposed a multiparametric score combining maximal WSS at the peak of the plaque associated with SWE texture analysis since the combined model scored a sensitivity of 80%, specificity of 78% and AUC of 0.8.

Mazzacaro et al. (88) found significantly higher YM in patients with stable plaques compared to those of vulnerable plaques (49.6 ± 8.1 kPa vs. 24.6 ± 4.3 kPa, p =.009). The PWV was similar (12.2 ± 0.9 m/s for stable plaques vs. 10.6 ± 0.5 m/s for vulnerable plaques (p =.16). Attempting to determine a cut-off elasticity value for plaque non-vulnerability, YM values >34 kPa had a sensitivity of 50% and a specificity of 73.3% and an AUC of 0.66.

The reliability of SWE in evaluating plaque stiffness and vulnerability was further validated by Wang et al. (70) reporting statistically significant differences in YM values among distinct echogenic types of plaques by whose plaque vulnerability was originally characterized (all $p < .05$).

5.4.3 SWE and Histology

In their novel study Garrard et al.(84), used histology as a reference method to assess plaque stability and independently identify features such as intraplaque hemorrhage and lipid presence. They found that an increasing number of foam cells and the presence of intra-plaque hemorrhage or thrombus were linked to a significantly lower YM (p =.049 and p = .043, respectively).

Zhang et al. (89) intended to compare the ultrasound findings with histopathological changes and to investigate the relationship between intraplaque neovascularization and plaque elasticity. Plaque neovascularization was negatively correlated with the SWV of SWE (p <.001), while the type I/III collagen ratio was significantly positively correlated with the SWV of SWE (p <.001). This added to the previous findings of Czernuszewicz et al. (90) who reported good performance for combined ARFI and stiff (AUC = 0.86) and soft (AUC = 0.89) categories.

In a comparative study (85) multiparametric ultrasound evaluation was performed in forty-three consecutive patients scheduled to undergo carotid endarterectomy. SWE identified 27 out of 31 plaques as vulnerable, demonstrating a sensitivity of 87.1% and a specificity of 66.7% when compared to histological findings. In contrast, a recent prospective observational study (87) reported significant overlap in stiffness values between histologically stable and vulnerable plaques, indicating that SWE alone might not be sufficient to distinguish between them.

The effectiveness of alternative ARFI-derived outcome parameters was investigated by Torres et al.(91), who reported that integrating both the correlation coefficient and

signal-to-noise ratio into a singular metric, log(VoA), significantly enhances the identification of carotid atherosclerotic plaque features, such as regions of collagen, calcification, lipid-rich necrotic core, and intraplaque hemorrhage, in comparison to ARFI peak displacement.

More recently Mazzacaro et al. (88) further support the correlation between YM when used to non-invasively quantify carotid plaque elasticity and histological characteristics, such as large IPH, ulceration, large necrotic/lipidic core, ruptured or thin fibrous cap, inflammatory cell infiltration, and neovascularization.

5.4.4 SWE and B-mode

In this pioneering study (76) the complementary use of ARFI to B-mode was already highlighted, since it can detect soft regions as small as 0.5 mm in diameter, which may not as easily resolved with B-mode imaging, while B-mode seems to remain preferable for IMT measurements. More recent studies (78,92,93) also underscore the potentially beneficial complementary role of SWE to classic B-mode ultrasound in assessing carotid plaque vulnerability.

Ramnarine et al. (77) reported that carotid plaque stiffness quantified by YM (AUC = 0.69) had better performance in predicting symptomatic carotid plaques when compared to Gray scale median (GSM) (AUC = 0.61). Both imaging modalities performed better when combined to percentage stenosis (AUC = 0.78 and 0.74, respectively). The potential advantage of SWE to B-mode is also pointed out by Li et al. (79) and Garrard et al. (84) due to the additional information provided by SWE, particularly tissue elasticity quantification.

In a pilot study (94) on 41 atheromatous lesions correlation was observed between SWE and Gray-Weale plaque classification method, which is consistent with Lou et al findings (78). Although, it should be pointed out that there was insufficient data to apply meaningful statistical correlation.

In a 2018 prospective comparative study Shang et al. (95), using SWV to measure elasticity, examined the correlation of SWE to the plaque echolucency. Echogenic plaques exhibited elevated shear wave velocities in comparison to echolucent plaques, whereas serum homocysteine concentrations demonstrated a negative correlation with the minimum, mean, and maximum values of SWV (all p values <.05)

More recently, Wang et al. (70) found statistically significant differences between GSM values (p <.001), with the maximum, mean, and minimum YM values of SWE (p < .001). Moreover, it revealed a positive association between plaque echotype, GSM, and YM (p <.001), indicating that a decrease in GSM corresponds to a reduction in echo and stiffness values. These findings add to other available literature (93) pointing out the statistically significant positive association of plaque echolucency and stiffness.

Popova et al. (96) in a 2024 prospective case-control study concerning elastographic evaluation of atherosclerotic plaques and assessment of vascular risk in individuals with rheumatoid arthritis (RA) investigated the SWE cut-off value for predicting plaque rupture and found that optimal cut-off value of 2D-SWE > 32.40 kPa was associated with a sensitivity of 96%, a specificity of 56%, a positive predictive value of 66.70%, and a negative predictive value of 92.90%. In the RA group, 2D-SWE values showed significant positive correlations with the severity of atherosclerotic plaques (p =.023) and the degree of stenosis (p <.001). Also, SWE showed a significant area under the curve (AUC = 0.818; 95% CI: 0.683 to 0.913; p <.001) and found significantly higher median values in the RA group when compared to the healthy group (p =.011).

5.4.5 SWE and MRI

Doherty et al. (92) compares, in a preliminary in vivo study, measures of carotid plaque stiffness obtained from ARFI imaging with its composition assessed through spatially registered MRI in five subjects exhibiting stenosis greater than 50%. The results support the potential of ARFI imaging to noninvasively identify vulnerable plaques, providing early evidence for its clinical utility. Normal loose matrix components appeared as homogeneous, stiff regions exhibiting little displacement in ARFI, while MRI identified calcium components were indistinguishable in ARFI. Lipid pools identified via MRI appeared as softer areas exhibiting about 1.8 times greater displacement in ARFI compared to adjacent stiffer regions.

In a 2020 study (97) MRI was employed for plaque classification and 410 SWE acquisitions were performed in 27 carotid plaques from 20 patients. AHA type VI plaques exhibited significantly higher group velocity compared to other types. Group and phase shear wave velocities were correlated with plaque characteristics such as

lipid-rich necrotic core content and IPH, suggesting that SWE can enhance plaque risk stratification.

Zhang et al. (86) in a retrospective observational study compared the diagnostic efficacy of SWE, AngioPLUS planewave ultrasensitive imaging (AP), and high-resolution MRI among 100 subjects. SWE and MRI results were similar demonstrating a sensitivity of 87.10%, 88.71% and a specificity of 76.32%, 78.95%, respectively. AP technology demonstrated the highest sensitivity (93.55%) and specificity (84.21%).

5.4.6 SWE and CEUS

Di Leo et al. (85) in 2018 were the first to compare SWE to CEUS in this novel study. SWE demonstrated a higher degree of agreement with CTA (81.4%) than with CEUS (74.4%). The AUC for SWE is 76.9%, surpassing CEUS's 72.7%, indicating superior overall diagnostic efficacy for SWE. Both SWE and CEUS had the same sensitivity (87.1%), which is comparable to CTA, while SWE demonstrated higher specificity (66,7%) than CEUS (58,3%).

In a 2021 study (89) on 94 individuals who had endarterectomy for symptomatic carotid artery stenosis showed that, the SWE value of the carotid plaque in hyper-enhancement areas were higher than that in hypoenhancement areas, of heterogeneously enhanced plaques. Also, there was a significant negative correlation between the SWV of SWE and the AUC of CEUS ($p < .001$), highlighting that assessments can occur simultaneously, facilitating both direct comparisons between elasticity and intraplaque neovascularization (IPN) thus ensuring efficiency, due to the ability to combine the two techniques utilizing the same probe and equipment.

Chen et al. (83) also suggests that the combination of multiple ultrasound modalities, such as CEUS and SWE, is viable and valuable for a thorough assessment of carotid plaque vulnerability and stroke risk, since the risk of stroke is significantly associated with IPN and SWV.

A most recent study (98) concerning 121 subjects with mild carotid stenosis (<50%) showed that the combination of IPN and SWV had better predictive value for the risk of stroke, since their combined methods model demonstrated a significantly better predictive performance ($p = .027$) when compared to grade 2 IPN or SWV methods alone.

5.5 Meta-analysis

5.5.1 Symptomatic Vs Asymptomatic

The pooled Standardized Mean Difference (SMD) is -0.89 with a 95% Confidence Interval (CI) of [-1.28, -0.50], which does not include zero. This indicates a statistically significant difference in elasticity between symptomatic and asymptomatic plaques. The negative SMD value demonstrates that asymptomatic plaques have higher elasticity, while symptomatic plaques have lower elasticity values, a finding that aligns with the pathophysiological differences between these types of plaques. The overall p-value for the test of $\theta = 0$ is $p < .001$, confirming statistical significance. Most individual studies (e.g., Rammnarine et al., Lou et al., Yi Li et al., Chen et al.) show statistically significant differences, as their CIs do not overlap zero. One study (Školoudík et al.) has a CI that includes zero, suggesting no statistical significance for that specific study. The heterogeneity statistics (I^2 = 73.37%) indicate substantial variability among studies. Despite this, the random-effects model has appropriately accounted for this variation in the pooled analysis as shown in *Figure 4.*

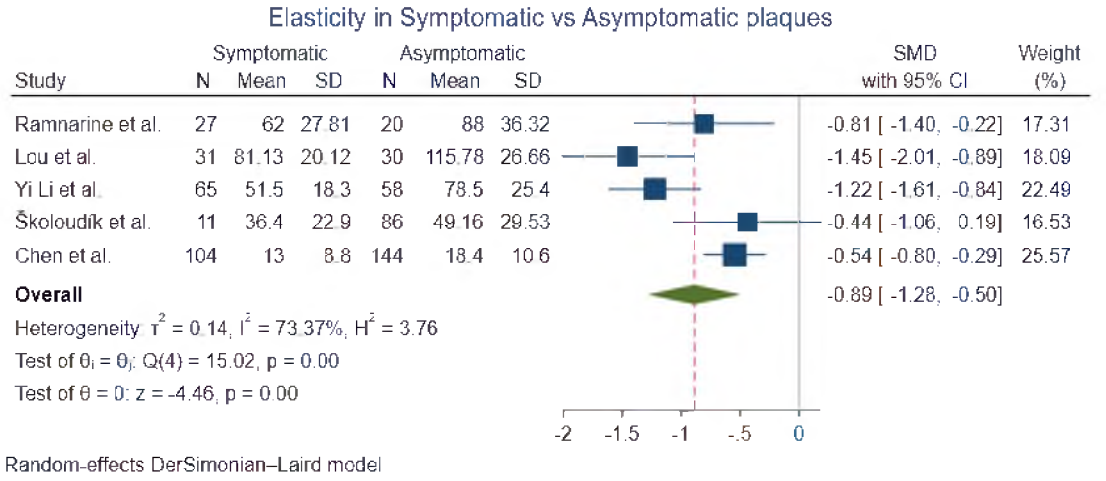

Figure 4 – Symptomatic Vs Asymptomatic Forest plot

5.5.2 Vulnerable vs Stable

The pooled Standardized Mean Difference (SMD) is -2.38 with a 95% Confidence Interval (CI) of [-3.68, -1.07]. Since the CI does not include zero, this indicates a statistically significant difference in elasticity between vulnerable and stable

plaques. There is a statistically significant difference in elasticity between vulnerable and stable plaques, with stable plaques exhibiting higher elasticity and vulnerable plaques showing lower elasticity values, schematically presented in the *Figure 5*. The test of $\theta = 0$ shows a p-value <.001, confirming that the difference is statistically significant. All individual studies (Garrard et al., Mazzaccaro et al., Wang et al.) show statistically significant differences, as their CIs do not overlap zero. The heterogeneity statistic ($I^2 = 91.51\%$) indicates high variability among the included studies, thus using a random-effects model for this meta-analysis was essential.

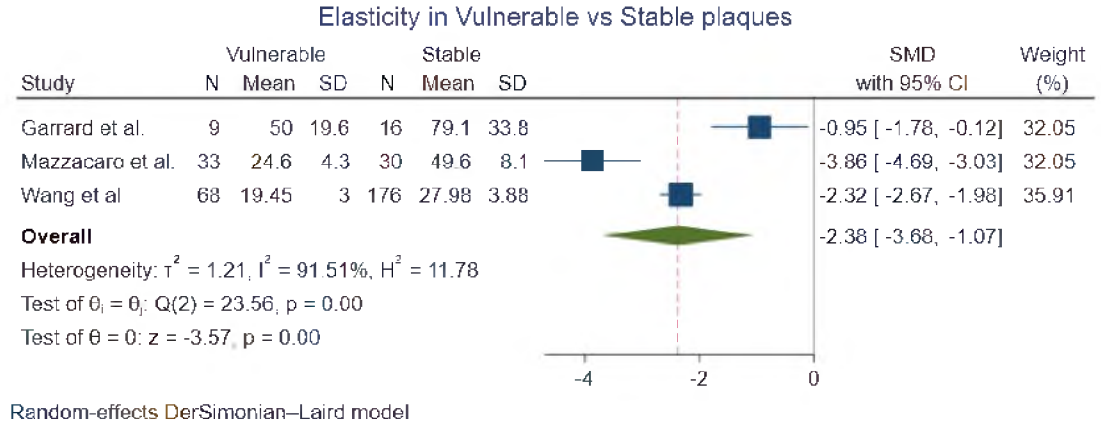

Figure 5 – Vulnerable Vs Stable Forest plot

5.6 Discussion

In this systematic review and meta-analysis, we approached the role of quantification of the carotid plaque's composition and the subsequent classification of the plaque as unstable or stable prior to the occurrence of a stroke.

Vulnerable or "soft" are distinguished by their increased lipid core content, propensity for hemorrhage, and ability to form thrombus (92). These exhibit lower YM or SWV values. On the other hand, stable or "stiff" plaques are histologically characterized by increased fibrous material and calcification, appear echogenic on conventional ultrasonography, and have higher YM or SWV values (90).

The capabilities of SWE ultrasound for detecting soft regions as small as 0.5 mm in diameter have already been shown (76). Recent studies (78,92,93) also highlight the potential benefits of SWE when combined with B-mode ultrasound in assessing carotid plaque vulnerability.

Combining multiple ultrasound modalities such as CEUS and SWE are valuable for assessing carotid plaque vulnerability and stroke risk. The combination of IPN and SWV as indexes for each method has already been tested and found feasible and valuable due to the ability assessing them simultaneously (83,89,98).

The ability of SWE to be comparable to established diagnostic methods, such as CTA (85) and MRI (86) indicate its potential. Furthermore, the significant advantages of vascular ultrasound imaging over CTA and MRI, which provide accurate identification and evaluation of vessels, are evident when considering the well-known benefits of ultrasound imaging, such as bedside availability, short examination times, lack of radiation exposure, and low cost (99).

As other studies (69,100) also pointed out cut-off values have not been yet established for YM and SWV and remain essential for SWE to gain its full potential as a diagnostic tool for carotid plaque assessment.

The findings of our meta-analysis study indicate statistically significant lower values of YM for vulnerable vs stable plaques and symptomatic vs asymptomatic plaques ($p<.001$ for both), further strengthening the hypothesis that vulnerable carotid plaques, which have the tendency to cause stroke, have lower elasticity values in terms of kPa.

Several limitations associated with this study should be pointed out. The heterogeneity of the included studies in terms of the type and scope of the study, the number of patients, the ultrasound devices and settings used, the number of measurements, the test location, the methods of comparison, and the type of reported data significantly complicated the comparison of the various studies included.

In conclusion, SWE showed promising results and poses great potential as a method for carotid plaque assessment and stroke risk stratification. Extended prospective multicenter clinical studies are deemed advantageous to determine the optimal technique and parameters to establish criteria and cut-off values for both the YM and SWV indexes of vulnerable plaques, thus giving us an advantage in stroke prevention and treatment.

6. BIBLIOGRAPHY

1. Feigin VL, Stark BA, Johnson CO, Roth GA, Bisignano C, Abady GG, et al. Global, regional, and national burden of stroke and its risk factors, 1990–2019: a systematic analysis for the Global Burden of Disease Study 2019. The Lancet Neurology. 2021 Oct 1;20(10):795–820.

2. eClinicalMedicine. The rising global burden of stroke. eClinicalMedicine [Internet]. 2023 May 1 [cited 2024 Oct 22];59. Available from: https://www.thelancet.com/journals/eclinm/article/PIIS2589-5370(23)00205-5/fulltext

3. World Stroke Organization (WSO): Global Stroke Fact Sheet 2022 - Valery L Feigin, Michael Brainin, Bo Norrving, Sheila Martins, Ralph L Sacco, Werner Hacke, Marc Fisher, Jeyaraj Pandian, Patrice Lindsay, 2022 [Internet]. [cited 2024 Oct 22]. Available from: https://journals.sagepub.com/doi/10.1177/17474930211065917

4. Naylor R, Rantner B, Ancetti S, de Borst GJ, De Carlo M, Halliday A, et al. Editor's Choice - European Society for Vascular Surgery (ESVS) 2023 Clinical Practice Guidelines on the Management of Atherosclerotic Carotid and Vertebral Artery Disease. Eur J Vasc Endovasc Surg. 2023 Jan;65(1):7–111.

5. Wafa HA, Wolfe CD, Emmett E, Roth GA, Johnson CO, Wang Y. Burden of Stroke in Europe: Thirty-Year Projections of Incidence, Prevalence, Deaths, and Disability-Adjusted Life Years. Stroke. 2020 Jul 10;51(8):2418.

6. Faateh M, Dakour-Aridi H, Mathlouthi A, Locham S, Naazie I, Malas M. Comparison of open- and closed-cell stent design outcomes after carotid artery stenting in the Vascular Quality Initiative. Journal of Vascular Surgery. 2021 May 1;73(5):1639–48.

7. Sacco RL, Kasner SE, Broderick JP, Caplan LR, Connors JJB, Culebras A, et al. An updated definition of stroke for the 21st century: a statement for healthcare professionals from the American Heart Association/American Stroke Association. Stroke. 2013 Jul;44(7):2064–89.

8. Groff H, Yousfani S, Pantoja-Ruiz C, Douiri A, Bhalla A, Wolfe C, et al. A systematic review of the incidence and outcomes of ICD-11 defined stroke. Journal of Stroke and Cerebrovascular Diseases [Internet]. 2024 Aug 1 [cited 2024 Oct 22];33(8). Available from: https://www.strokejournal.org/article/S1052-3057(24)00229-5/fulltext

9. Mbonde AA, O'Carroll CB, Dulamea OA, Anghel D, Chong BW, Dumitrascu OM. Current Guidelines on Management of Amaurosis Fugax and Transient Ischemic Attacks. Asia-Pacific Journal of Ophthalmology. 2022 Mar 1;11(2):168–76.

10. Guntel M, Guntel M. https://services.igi-global.com/resolvedoi/resolve.aspx?doi=10.4018/978-1-7998-7433-1.ch010. IGI Global; 1AD [cited 2024 Oct 22]. Transient Ischemic Attack. Available from: https://www.igi-global.com/gateway/chapter/www.igi-global.com/gateway/chapter/294598

11. Moini J, Gutierrez A, Avgeropoulos N. Chapter 10 - Stroke. In: Moini J, Gutierrez A, Avgeropoulos N, editors. Clinical Neuroepidemiology of Acute and Chronic Disorders [Internet]. Academic Press; 2023 [cited 2024 Oct 22]. p. 153–68. Available from: https://www.sciencedirect.com/science/article/pii/B978032395901800002X

12. Charlick M, Das JM. Anatomy, Head and Neck: Internal Carotid Arteries. In: StatPearls [Internet]. Treasure Island (FL): StatPearls Publishing; 2024 [cited 2024 Nov 17]. Available from: http://www.ncbi.nlm.nih.gov/books/NBK556061/

13. Milutinović A, Šuput D, Zorc-Pleskovič R. Pathogenesis of atherosclerosis in the tunica intima, media, and adventitia of coronary arteries: An updated review. Biomolecules and Biomedicine. 2020 Feb 5;20(1):21–30.

14. Sluiter TJ, van Buul JD, Huveneers S, Quax PHA, de Vries MR. Endothelial Barrier Function and Leukocyte Transmigration in Atherosclerosis. Biomedicines. 2021 Mar 24;9(4):328.

15. Malekmohammad K, Sewell RDE, Rafieian-Kopaei M. Antioxidants and Atherosclerosis: Mechanistic Aspects. Biomolecules. 2019 Jul 25;9(8):301.

16. Humphrey JD, Schwartz MA. Vascular Mechanobiology: Homeostasis, Adaptation, and Disease. Annu Rev Biomed Eng. 2021 Jul 13;23:1–27.

17. Zhou M, Yu Y, Chen R, Liu X, Hu Y, Ma Z, et al. Wall shear stress and its role in atherosclerosis. Front Cardiovasc Med [Internet]. 2023 Apr 3 [cited 2024 Nov 17];10. Available from: https://www.frontiersin.org/journals/cardiovascular-medicine/articles/10.3389/fcvm.2023.1083547/full

18. Roux E, Bougaran P, Dufourcq P, Couffinhal T. Fluid Shear Stress Sensing by the Endothelial Layer. Front Physiol [Internet]. 2020 Jul 24 [cited 2024 Nov 17];11. Available from: https://www.frontiersin.org/journals/physiology/articles/10.3389/fphys.2020.00861/full

19. Ahmadpour-B M, Nooraeen A, Tafazzoli-Shadpour M, Taghizadeh H. Contribution of atherosclerotic plaque location and severity to the near-wall hemodynamics of the carotid bifurcation: an experimental study and FSI modeling. Biomech Model Mechanobiol. 2021 Jun;20(3):1069–85.

20. Prasad K, Kalra J. Oxygen free radicals and hypercholesterolemic atherosclerosis: effect of vitamin E. Am Heart J. 1993 Apr;125(4):958–73.

21. Prasad K, Kalra J, Lee P. Oxygen free radicals as a mechanism of hypercholesterolemic atherosclerosis: Effects of probucol. International Journal of Angiology. 1994 Mar 1;3(1):100–12.

22. Willam C, Schindler R, Frei U, Eckardt KU. Increases in oxygen tension stimulate expression of ICAM-1 and VCAM-1 on human endothelial cells. American Journal of Physiology-Heart and Circulatory Physiology. 1999 Jun;276(6):H2044–52.

23. Martin A, Foxall T, Blumberg JB, Meydani M. Vitamin E Inhibits Low-Density Lipoprotein–Induced Adhesion of Monocytes to Human Aortic Endothelial Cells In Vitro. Arteriosclerosis, Thrombosis, and Vascular Biology. 1997 Mar;17(3):429–36.

24. Fraticelli A, Serrano CV, Bochner BS, Capogrossi MC, Zweier JL. Hydrogen peroxide and superoxide modulate leukocyte adhesion molecule expression and leukocyte endothelial adhesion. Biochimica et Biophysica Acta (BBA) - Molecular Cell Research. 1996 Feb 29;1310(3):251–9.

25. Cushing SD, Berliner JA, Valente AJ, Territo MC, Navab M, Parhami F, et al. Minimally modified low density lipoprotein induces monocyte chemotactic protein 1 in human endothelial cells and smooth muscle cells. Proceedings of the National Academy of Sciences. 1990 Jul;87(13):5134–8.

26. Steinberg D. Oxidized low density lipoprotein--an extreme example of lipoprotein heterogeneity. Isr J Med Sci. 1996 Jun;32(6):469–72.

27. Hashimoto K, Kataoka N, Nakamura E, Tsujioka K, Kajiya F. Oxidized LDL specifically promotes the initiation of monocyte invasion during transendothelial migration with upregulated PECAM-1 and downregulated VE-cadherin on endothelial junctions. Atherosclerosis. 2007 Oct;194(2):e9-17.

28. Phan SH, McGarry BM, Loeffler KM, Kunkel SL. Regulation of Macrophage-Derived Fibroblast Growth Factor Release by Arachidonate Metabolites. Journal of Leukocyte Biology. 1987 Aug 1;42(2):106–13.

29. Prasad K. Pathophysiology and Medical Treatment of Carotid Artery Stenosis. The International Journal of Angiology : Official Publication of the International College of Angiology, Inc. 2015 Jun 23;24(3):158.

30. Goessens BMB, Visseren FLJ, Kappelle LJ, Algra A, van der Graaf Y. Asymptomatic carotid artery stenosis and the risk of new vascular events in patients with manifest arterial disease: the SMART study. Stroke. 2007 May;38(5):1470–5.

31. Conrad MF, Michalczyk MJ, Opalacz A, Patel VI, LaMuraglia GM, Cambria RP. The natural history of asymptomatic severe carotid artery stenosis. J Vasc Surg. 2014 Nov;60(5):1218–26.

32. Ferguson GG, Eliasziw M, Barr HW, Clagett GP, Barnes RW, Wallace MC, et al. The North American Symptomatic Carotid Endarterectomy Trial : surgical results in 1415 patients. Stroke. 1999 Sep;30(9):1751–8.

33. Walker MD, Marler JR, Goldstein M, Grady PA, Toole JF, Baker WH, et al. Endarterectomy for Asymptomatic Carotid Artery Stenosis. JAMA. 1995 May 10;273(18):1421–8.

34. Halliday A, Harrison M, Hayter E, Kong X, Mansfield A, Marro J, et al. 10-year stroke prevention after successful carotid endarterectomy for asymptomatic stenosis (ACST-1): a multicentre randomised trial. Lancet. 2010 Sep 25;376(9746):1074–84.

35. Doonan RJ, Gorgui J, Veinot JP, Lai C, Kyriacou E, Corriveau MM, et al. Plaque echodensity and textural features are associated with histologic carotid plaque instability. J Vasc Surg. 2016 Sep;64(3):671-677.e8.

36. Baradaran H, Gialdini G, Mtui E, Askin G, Kamel H, Gupta A. Silent Brain Infarction in Patients With Asymptomatic Carotid Artery Atherosclerotic Disease. Stroke. 2016 Dec;47(5):1368–70.

37. Markus HS, King A, Shipley M, Topakian R, Cullinane M, Reihill S, et al. Asymptomatic embolisation for prediction of stroke in the Asymptomatic Carotid Emboli Study (ACES): a prospective observational study. Lancet Neurol. 2010 Jul;9(7):663–71.

38. Cicha I, Wörner A, Urschel K, Beronov K, Goppelt-Struebe M, Verhoeven E, et al. Carotid Plaque Vulnerability. Stroke. 2011 Dec;42(12):3502–10.

39. Yilmaz A, Lipfert B, Cicha I, Schubert K, Klein M, Raithel D, et al. Accumulation of immune cells and high expression of chemokines/chemokine receptors in the upstream shoulder of atherosclerotic carotid plaques. Experimental and Molecular Pathology. 2007 Jun 1;82(3):245–55.

40. Butcovan D, Mocanu V, Baran D, Ciurescu D, Tinica G. Assessment of vulnerable and unstable carotid atherosclerotic plaques on endarterectomy specimens. Exp Ther Med. 2016 Dec;11(5):2028–32.

41. van der Wal AC, Becker AE. Atherosclerotic plaque rupture--pathologic basis of plaque stability and instability. Cardiovasc Res. 1999 Feb;41(2):334–44.

42. Li J, Wu H, Hao Y, Yao X. Unstable Carotid Plaque is Associated With Coagulation Function and Platelet Activity Evaluated by Thrombelastography. J Stroke Cerebrovasc Dis. 2019 Nov;28(11):104336.

43. Imbesi SG, Kerber CW. Why do ulcerated atherosclerotic carotid artery plaques embolize? A flow dynamics study. AJNR Am J Neuroradiol. 1998 Apr;19(4):761–6.

44. Redgrave JNE, Lovett JK, Gallagher PJ, Rothwell PM. Histological assessment of 526 symptomatic carotid plaques in relation to the nature and timing of ischemic symptoms: the Oxford plaque study. Circulation. 2006 Dec 16;113(19):2320–8.

45. Nandalur KR, Hardie AD, Raghavan P, Schipper MJ, Baskurt E, Kramer CM. Composition of the stable carotid plaque: insights from a multidetector computed tomography study of plaque volume. Stroke. 2007 Mar;38(3):935–40.

46. Tegos TJ, Sohail M, Sabetai MM, Robless P, Akbar N, Pare G, et al. Echomorphologic and histopathologic characteristics of unstable carotid plaques. AJNR Am J Neuroradiol. 2000;21(10):1937–44.

47. Mofidi R, Green BR, Mofidi R, Green BR. Carotid Plaque Morphology: Plaque Instability and Correlation with Development of Ischaemic Neurological Events. In: Carotid Artery Disease - From Bench to Bedside and Beyond [Internet]. IntechOpen; 2014 [cited 2024 Oct 21]. Available from: https://www.intechopen.com/chapters/45982

48. Moulton KS, Vakili K, Zurakowski D, Soliman M, Butterfield C, Sylvin E, et al. Inhibition of plaque neovascularization reduces macrophage accumulation and progression of advanced atherosclerosis. Proc Natl Acad Sci U S A. 2003 Apr 15;100(8):4736–41.

49. de Boer OJ, van der Wal AC, Teeling P, Becker AE. Leucocyte recruitment in rupture prone regions of lipid-rich plaques: a prominent role for neovascularization? Cardiovasc Res. 1999 Feb;41(2):443–9.

50. Badimon L, Vilahur G. Thrombosis formation on atherosclerotic lesions and plaque rupture. J Intern Med. 2014 Dec;276(6):618–32.

51. Schmidt C, Fischer T, Rückert RI, Oberwahrenbrock T, Harms L, Kronenberg G, et al. Identification of neovascularization by contrast–enhanced ultrasound to detect unstable carotid stenosis. PLOS ONE. 2017;12(4):e0175331.

52. Gray-Weale AC, Graham JC, Burnett JR, Byrne K, Lusby RJ. Carotid artery atheroma: comparison of preoperative B-mode ultrasound appearance with carotid endarterectomy specimen pathology. J Cardiovasc Surg (Torino). 1988;29(6):676–81.

53. Geroulakos G, Ramaswami G, Nicolaides A, James K, Labropoulos N, Belcaro G, et al. Characterization of symptomatic and asymptomatic carotid plaques using high-resolution real-time ultrasonography. Br J Surg. 1993 Oct;80(10):1274–7.

54. Stary HC, Chandler AB, Dinsmore RE, Fuster V, Glagov S, Insull W, et al. A Definition of Advanced Types of Atherosclerotic Lesions and a Histological Classification of Atherosclerosis. Circulation. 1995 Sep;92(5):1355–74.

55. Cai JM, Hatsukami TS, Ferguson MS, Small R, Polissar NL, Yuan C. Classification of Human Carotid Atherosclerotic Lesions With In Vivo Multicontrast Magnetic Resonance Imaging. Circulation. 2002 Sep 10;106(11):1368–73.

56. Sarvazyan A, Hall TJ, Urban MW, Fatemi M, Aglyamov SR, Garra BS. An Overview of Elastography-An Emerging Branch of Medical Imaging. Current Medical Imaging. 7(4):255–82.

57. Gennisson JL, Deffieux T, Fink M, Tanter M. Ultrasound elastography: Principles and techniques. Diagnostic and Interventional Imaging. 2013 May 1;94(5):487–95.

58. Cui XW, Li KN, Yi AJ, Wang B, Wei Q, Wu GG, et al. Ultrasound elastography. Endoscopic Ultrasound. 2022 Aug;11(4):252.

59. Bamber J, Cosgrove D, Dietrich CF, Fromageau J, Bojunga J, Calliada F, et al. EFSUMB Guidelines and Recommendations on the Clinical Use of Ultrasound Elastography. Part 1: Basic Principles and Technology. Ultraschall in der Medizin - European Journal of Ultrasound. 2013 Apr 4;34:169–84.

60. Dietrich CF, Dong Y, Cui XW, Fink M, Jenssen C, Moeller K, et al. Ultrasound elastography: a brief clinical history of an evolving technique. Ultrasound Int Open. 2024 Oct 9;10(CP):a-2378-6926.

61. Cè M, D'Amico NC, Danesini GM, Foschini C, Oliva G, Martinenghi C, et al. Ultrasound Elastography: Basic Principles and Examples of Clinical Applications with Artificial Intelligence—A Review. BioMedInformatics. 2023 Mar;3(1):17–43.

62. Yamashita Y, Kitano M. Benefits and limitations of each type of endoscopic ultrasonography elastography technology for diagnosis of pancreatic diseases. Digestive Endoscopy. 2021;33(4):554–6.

63. Shiina T, Nightingale KR, Palmeri ML, Hall TJ, Bamber JC, Barr RG, et al. WFUMB Guidelines and Recommendations for Clinical Use of Ultrasound Elastography: Part 1: Basic Principles and Terminology. Ultrasound in Medicine and Biology. 2015 May 1;41(5):1126–47.

64. Wells PNT, Liang HD. Medical ultrasound: imaging of soft tissue strain and elasticity. J R Soc Interface. 2011 Nov 7;8(64):1521–49.

65. Mazzaccaro D, Malacrida G, Amato B, Angileri SA, Ierardi AM, Nano G. Preliminary experience with the use of ultra-low profile endografts. Diagnostic and Interventional Radiology. 2017 Nov 1;23(6):448–53.

66. Tanter M, Bercoff J, Sandrin L, Fink M. Ultrafast compound imaging for 2-D motion vector estimation: application to transient elastography. IEEE Trans Ultrason Ferroelectr Freq Control. 2002 Oct;49(10):1363–74.

67. Dietrich CF, Bamber J, Berzigotti A, Bota S, Cantisani V, Castera L, et al. EFSUMB Guidelines and Recommendations on the Clinical Use of Liver Ultrasound Elastography, Update 2017 (Short Version). Ultraschall in der Medizin - European Journal of Ultrasound. 2017 Apr 13;38:377–94.

68. Flaherty ML, Kissela B, Khoury JC, Alwell K, Moomaw CJ, Woo D, et al. Carotid Artery Stenosis as a Cause of Stroke. Neuroepidemiology. 2012 Oct 11;40(1):36–41.

69. Mbroh J, Tünnerhoff J, Poli K, Bender B, Schwarz P, Mengel A, et al. Shear Wave Elastography for the Assessment of Carotid Plaque Vulnerability: A Systematic Review. Acta Neurologica Scandinavica. 2023;2023(1):5084699.

70. Wang B, Chen Y, Qiao Q, Dong L, Xiao C, Qi Z. Evaluation of carotid plaque vulnerability with different echoes by shear wave elastography and CEUS. Journal of Stroke and Cerebrovascular Diseases [Internet]. 2023 Mar 1 [cited 2024 Oct 20];32(3). Available from: https://www.strokejournal.org/article/S1052-3057(22)00633-4/abstract

71. Bulum A, Ivanac G, Mandurić F, Pfeifer L, Bulum M, Divjak E, et al. Contribution of UltraFast™ Ultrasound and Shear Wave Elastography in the Imaging of Carotid Artery Disease. Diagnostics. 2022 May;12(5):1168.

72. Page MJ, McKenzie JE, Bossuyt PM, Boutron I, Hoffmann TC, Mulrow CD, et al. The PRISMA 2020 statement: an updated guideline for reporting systematic reviews. BMJ. 2021 Mar 29;372:n71.

73. Wan X, Wang W, Liu J, Tong T. Estimating the sample mean and standard deviation from the sample size, median, range and/or interquartile range. BMC Medical Research Methodology. 2014 Dec 19;14(1):135.

74. Higgins JPT, Thomas J, Chandler J, Cumpston M, Li T, Page MJ, Welch VA (editors). Cochrane Handbook for Systematic Reviews of Interventions version 6.5 (updated August 2024). Cochrane, 2024. [Internet]. Available from: https://training.cochrane.org/handbook

75. DerSimonian R, Laird N. Meta-analysis in clinical trials. Controlled Clinical Trials. 1986 Sep 1;7(3):177–88.

76. Dahl JJ, Dumont DM, Allen JD, Miller EM, Trahey GE. ACOUSTIC RADIATION FORCE IMPULSE IMAGING FOR NONINVASIVE CHARACTERIZATION OF CAROTID ARTERY

ATHEROSCLEROTIC PLAQUES: A FEASIBILITY STUDY. Ultrasound in medicine & biology. 2009 Feb 25;35(5):707.

77. Ramnarine KV, Garrard JW, Kanber B, Nduwayo S, Hartshorne TC, Robinson TG. Shear wave elastography imaging of carotid plaques: feasible, reproducible and of clinical potential. Cardiovasc Ultrasound. 2014 Dec 8;12:49.

78. Lou Z, Yang J, Tang L, Jin Y, Zhang J, Liu C, et al. Shear Wave Elastography Imaging for the Features of Symptomatic Carotid Plaques: A Feasibility Study. J Ultrasound Med. 2017 Jun;36(6):1213–23.

79. Li Y, Zheng S, Zhang J, Wang F, Liu X, He W. Advance ultrasound techniques for the assessment of plaque vulnerability in symptomatic and asymptomatic carotid stenosis: a multimodal ultrasound study. Cardiovasc Diagn Ther. 2021 Feb;11(1):28–38.

80. Sivasankar R, Singh R, Hashim PI, Soni BK, Patel RK, Bajpai A. Evaluation of Carotid Plaque Vulnerability Using Shear-Wave Elastography: An Observational Comparative Study. Journal of Marine Medical Society. 2019 Dec;21(2):134.

81. Školoudík D, Kešnerová P, Vomáčka J, Hrbáč T, Netuka D, Forostyak S, et al. Shear-Wave Elastography Enables Identification of Unstable Carotid Plaque. Ultrasound Med Biol. 2021 Jul;47(7):1704–10.

82. Globa MV, Derkach BV. Modern approaches to ultrasonographic assessment of carotid plaque in terms of its potential instability. Wiad Lek. 2024;77(5):919–25.

83. Chen J, Wang B, Song J, Qi Z, Deng Y. Multiple techniques to evaluate the relationship between carotid artery plaque and acute stroke. Clinical Hemorheology and Microcirculation. 2024 Jan 1;86(3):327–37.

84. Garrard JW, Ummur P, Nduwayo S, Kanber B, Hartshorne TC, West KP, et al. Shear Wave Elastography May Be Superior to Greyscale Median for the Identification of Carotid Plaque Vulnerability: A Comparison with Histology. Ultraschall Med. 2015 Aug;36(4):386–90.

85. Di Leo N, Venturini L, de Soccio V, Forte V, Lucchetti P, Cerone G, et al. Multiparametric ultrasound evaluation with CEUS and shear wave elastography for carotid plaque risk stratification. J Ultrasound. 2018 Dec;21(4):293–300.

86. Zhang S, Jiang S, Wang C, Han C. Comparison of ultrasonic shear wave elastography, AngioPLUS planewave ultrasensitive imaging, and optimized high-resolution magnetic resonance imaging in evaluating carotid plaque stability. PeerJ. 2023 Sep 27;11:e16150.

87. Goudot G, Sitruk J, Jimenez A, Khider L, Julia P, Alsac JM, et al. Carotid plaque vulnerability assessed by combined shear wave elastography and ultrafast doppler compared to histology: the UF-plaque study. European Heart Journal. 2021 Oct 1;42(Supplement_1):ehab724.1995.

88. Mazzaccaro D, Giannetta M, Fancoli F, Matrone G, Curcio N, Conti M, et al. Role of Preoperative Ultrasound Shear-Wave Elastography and Radiofrequency-Based Arterial Wall Tracking in Assessing the Vulnerability of Carotid Plaques: Preliminary Results. Diagnostics. 2023 Jan;13(4):805.

89. Zhang Y, Cao J, Zhou J, Zhang C, Li Q, Chen S, et al. Plaque Elasticity and Intraplaque Neovascularisation on Carotid Artery Ultrasound: A Comparative Histological Study. Eur J Vasc Endovasc Surg. 2021 Sep;62(3):358–66.

90. Czernuszewicz TJ, Homeister JW, Caughey MC, Wang Y, Zhu H, Huang BY, et al. Performance of acoustic radiation force impulse ultrasound imaging for carotid plaque characterization with histologic validation. Journal of Vascular Surgery. 2017 Dec 1;66(6):1749-1757.e3.

91. Torres G, Czernuszewicz TJ, Homeister JW, Caughey MC, Huang BY, Lee ER, et al. Delineation of Human Carotid Plaque Features In Vivo by Exploiting Displacement Variance. IEEE transactions on ultrasonics, ferroelectrics, and frequency control. 2019 Feb 11;66(3):481.

92. Doherty JR, Dahl JJ, Kranz PG, Husseini NE, Chang HC, Chen N kuei, et al. Comparison of Acoustic Radiation Force Impulse Imaging Derived Carotid Plaque Stiffness with Spatially Registered MRI Determined Composition. IEEE transactions on medical imaging. 2015 May 13;34(11):2354.

93. Lei Z, Qiang Y, Tianning P, Jie L. Quantitative assessment of carotid atherosclerotic plaque: Initial clinical results using ShearWave™ Elastography. International Journal of Clinical and Experimental Medicine. 2016;9(6):9347–55.

94. Carter M, Hall T, Baun J. Carotid Plaque Characterization Using Quantitative Shear Wave Elastography: A Pilot Study. Journal of Diagnostic Medical Sonography. 2022 May 1;38(3):257–62.

95. Shang J, Wang W, Feng J, Luo GG, Dang Y, Sun J, et al. Carotid Plaque Stiffness Measured with Supersonic Shear Imaging and Its Correlation with Serum Homocysteine Level in Ischemic Stroke Patients. Korean J Radiol. 2018;19(1):15–22.

96. Popova V, Popova-Belova S, Geneva-Popova M, Karalilova R, Batalov Z, Batalov K, et al. Elastographic Assessment of Atherosclerotic Plaques and Determination of Vascular Risk in Patients with Rheumatoid Arthritis. Diagnostics. 2024 Jan;14(21):2426.

97. Marlevi D, Mulvagh SL, Huang R, DeMarco JK, Ota H, Huston J, et al. Combined spatiotemporal and frequency-dependent shear wave elastography enables detection of vulnerable carotid plaques as validated by MRI. Sci Rep. 2020 Jan 15;10(1):403.

98. Zhang L, Jia C, Gu S, Chen J, Wu R. Intraplaque neovascularization combined with plaque elasticity for predicting ipsilateral stroke in patients with asymptomatic mild carotid stenosis. Quantitative Imaging in Medicine and Surgery. 2024 Jun 17;14(7):4815.

99. Golemati S, Cokkinos DD. Recent advances in vascular ultrasound imaging technology and their clinical implications. Ultrasonics. 2022 Feb 1;119:106599.

100. Davidhi A, Rafailidis V, Destanis E, Prassopoulos P, Foinitsis S. Ultrasound Elastography: another piece in the puzzle of carotid plaque vulnerability? Medical Ultrasonography. 2022 Aug 31;24(3):356–63.